

NATIONAL AERONAUTICS AND SPACE ADMINISTRATION

Technical Report 32-1228

*Tensile Creep Studies
on Glassy Carbon*

D. B. Fischbach

FF No. 602(C)	<u>N68-17390</u>		(THRU)
	(ACCESSION NUMBER)		
	<u>23</u>	(PAGES)	<u>1</u>
	(CODE)		
	<u>CF-93203</u>	(NASA CR OR TMX OR AD NUMBER)	<u>18</u>
			(CATEGORY)
AVAILABLE TO GOVERNMENT AGENCIES ONLY			

JET PROPULSION LABORATORY
CALIFORNIA INSTITUTE OF TECHNOLOGY
PASADENA, CALIFORNIA

March 1, 1968

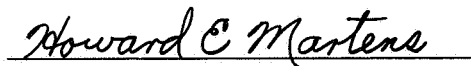
NATIONAL AERONAUTICS AND SPACE ADMINISTRATION

Technical Report 32-1228

*Tensile Creep Studies
on Glassy Carbon*

D. B. Fischbach

Approved by:



Howard E. Martens, Manager
Materials Section

JET PROPULSION LABORATORY
CALIFORNIA INSTITUTE OF TECHNOLOGY
PASADENA, CALIFORNIA

March 1, 1968

TECHNICAL REPORT 32-1228

Copyright © 1968
Jet Propulsion Laboratory
California Institute of Technology
Prepared Under Contract No. NAS 7-100
National Aeronautics & Space Administration

Acknowledgment

It is a pleasure to acknowledge the assistance of R. D. Ringstead and H. L. Wood in taking the data. G. M. Jenkins, M. H. Leipold and H. E. Martens provided helpful discussions.

Contents

I. Introduction	1
II. Experimental Materials and Techniques.	1
III. Results	5
IV. Discussion	9
V. Structure of Glassy Carbon	12
VI. Summary	14
References	14

Table

1. Gage section magnetic susceptibility anisotropy ratios	5
---	---

Figures

1. Modified grip assembly showing GC-30 inserts, specimen centering screws and PC clamping shims	3
2. Specimen configuration with ink fiducial marks, top, and observed distribution of deformation along specimen length, bottom	4
3. Reduction in cross-sectional area as a function of uniform gage elongation for GC-20 and GC-30	5
4. Portion of a typical elongation vs time curve showing stress changes	6
5. Recorded creep rate as a function of creep elongation (log-log coordinates) for a GC-30 specimen at several stress levels	7
6. Creep rate as a function of stress, from data of Fig. 5	8
7. The stress exponent n as a function of stress for GC-20 and GC-30	8
8. Typical elongation vs time curve showing creep recovery when load was removed	9
9. Recorded creep rate as function of elongation (log-log coordinates) for a GC-30 specimen at several temperatures	10
10. Arrhenius plot of creep rate vs reciprocal absolute temperature, from data of Fig. 9	11

Abstract

The tensile creep behavior of glassy carbon has been investigated at elevated temperatures for two grades of Japanese glassy carbon, GC-20 and GC-30, which had been heat-treated to maximum temperatures of 2000 and 3000°C respectively according to the manufacturer. Similar behavior was found for the two grades. The reduction in cross-sectional area of GC-30 was nearly that predicted for constant volume deformation; the reduction in area of GC-20 was a little smaller. A stress-change technique was used to determine the dependence of the isothermal creep rate on elongation at various stress levels. The creep rate decreased monotonically with elongation under constant load and temperature. The stress dependence of the creep rate, determined from these data, could be represented approximately by $\dot{\epsilon} = A\sigma^n$ where $n = 1 + B\sigma$ with $B = 3.7 \times 10^{-4} \text{ in.}^2/\text{lb}$ over the range 0–18,000 psi and 2500–2900°C. Tensile elongation produced a definite preferred orientation texture (layer planes aligned parallel to the stress axis) in the initially isotropic carbon. Creep recovery occurred when the stress was reduced. Although only a small amount of recovery resulted from small stress reductions, at least 25% of the creep elongation was recoverable when the stress was reduced nearly to zero. A temperature-change technique at constant load was used to determine the dependence of creep rate on elongation at various temperatures. The effective activation energy determined from these data is $350 \pm 40 \text{ kcal/mole}$ over the range 2500–2900°C and 6000–16,000 psi. A simple structural model for glassy carbon, inferred from the properties of this material, can account qualitatively for much of the observed behavior. However, more detailed and definitive information on structure will be required before the behavior can be explained with confidence.

Tensile Creep Studies on Glassy Carbon

I. Introduction

Glassy (vitreous) carbons are a type of synthetic carbon material characterized by low density, a relatively stable isotropic disordered structure and very low gas permeability (Refs. 1-4). Fractured surfaces are glass-like in appearance. These carbons belong to the interesting broad class of nongraphitizing carbons which includes many ablative chars and high performance carbon fibers among its members. A number of varieties of glassy carbon have been produced in the laboratory and several are commercially available. Detailed descriptions of the starting materials and preparation techniques have not been published in most cases. However, it is known that in general the process consists of the slow and carefully controlled pyrolysis of cross-linked thermosetting polymer resins (Refs. 5-8). Although the detailed preparation process undoubtedly varies, glassy carbons from different sources appear to have similar properties.

Previous tensile stress-strain studies here (Refs. 9-11) on commercial glassy carbons of Japanese manufacture showed that these carbons have very good high-temperature mechanical properties, especially on a strength per unit weight basis. Thus, they appear to have good potential for many high temperature applications.

They also are a suitable model material for studies on the behavior of nongraphitizing carbons. This report describes the results of an investigation of the high temperature tensile creep behavior of Japanese glassy carbon. Information was obtained on 1) the temperature and stress dependence of the creep rate, 2) creep recovery, and 3) the reduction in gage cross-sectional area associated with tensile elongation, among others.

II. Experimental Materials and Techniques

The glassy carbon was obtained from the manufacturer¹ in the form of flat plates measuring approximately $4 \times 4 \times 0.1$ in. Two grades of material, GC-20 and GC-30, which had been heat-treated to temperatures of 2000 and 3000°C respectively according to the manufacturer, were used. Only a few tests were run on GC-20 since earlier results (Refs. 9-11) had indicated that structural changes occurred in this material in the creep test temperature range 2500-2900°C. Most of the data was obtained on GC-30 which, because of its higher heat treatment temperature, had a structure that was stable in the test temperature range. Dog-bone type specimens

¹Tokai Electrode Manufacturing Company, Ltd.

with a uniform gage section measuring approximately $0.1 \times 0.075 \times 0.75$ in. and a 0.75-in. radius grip surface were cut and ground from these plates using diamond tooling. The corners generally had many small nicks and chips but these did not appear to affect the creep behavior significantly.

The general techniques and equipment used for the creep tests have been described in detail in previous reports (Refs. 12 and 13). Therefore, only a brief description will be given here with emphasis on recent modifications which are pertinent to the present investigation. The apparatus consists of a dead-weight constant load creep frame with an automatically controlled graphite tube resistance furnace, and recording extensometer and load cell. The furnace was capable of achieving temperatures $\geq 2900^\circ\text{C}$. Specimen temperatures were measured with a calibrated disappearing-filament optical pyrometer, and then they were corrected for window absorption. Tests were conducted with a helium atmosphere at approximately ambient pressure in the furnace.

The load train components within the furnace were made entirely of carbon or graphite. An improved version of the split-grip design which has been in use here for some time was employed. The disassembled grips are shown in Fig. 1. The grip halves and clamping rings were machined from a fine-grained coke-pitch graphite. The modifications consisted of GC-30 inserts which bridged the two grip halves and formed the loading surface; and threaded studs used to center the specimen in the grip cavity.² The GC-30 inserts were much harder and less ductile than the synthetic graphite grips and served the same purpose as carbide or hardened steel grip parts often used for tensile testing at more moderate temperatures. They effectively prevented uneven or eccentric specimen loading due to shear or separation of the grip halves and substantially reduced grip deformation. A jig was used for assembling the load train and a special clamp was used to support the grips and prevent damage to the specimen while the load train was being installed in or removed from the furnace. These techniques made it possible to handle these brittle specimens routinely without accidental breakage.

Dead-weight loads were applied and removed using a ball-screw jack. A special weight pan was used to apply

the load in two increments of variable size for the stress dependence studies. The load train was suspended from a load cell attached to the top of the creep frame. It was sealed to the furnace with a sleeve of thin rubber sheet at the top and a rubberized fabric bellows at the bottom. Between the bottom of the furnace and the attachment of the weight pan was a guide bearing. The load train itself applied a tare weight to the specimen of about 4.6 lb (approximately 500 psi).

Specimen elongation was recorded by sensing changes in the separation of the grips with an external strain-gage bridge extensometer coupled to the grips with $\frac{1}{8}$ -in.-diam carbon rods. The extensometer was calibrated relative to the uniform gage length of the specimens. However, since grip separation was actually measured, the recorded elongation included an appreciable contribution from elongation of the throat sections at each end of the gage section, and much smaller contributions from deformation of the grip portion of the specimen and of the grips themselves, and changes in alignment of the grips on loading. Fiducial marks were drawn on the specimen, with black acetate drawing ink, to determine the true uniform gage section elongation and the distribution of deformation along the specimen length. These black ink lines were clearly distinguishable against the dark grey color of the specimen and survived temperatures of at least 2900°C . Measurement with a traveling microscope of the distances between adjacent lines before and after deformation gave the desired information. A sketch of the specimen showing the location of the ink lines is shown at the top of Fig. 2, and the distribution of deformation after a recorded plastic creep elongation of 16% is shown at the bottom of Fig. 2. The elongation was found to be approximately uniform in the gage section and to fall off as the grip regions were approached in the manner expected for the specimen shape. The uniform gage elongation was found to be approximately $\frac{2}{3}$ of the recorded elongation. The recorded creep rates reported here should be multiplied by this factor to get approximate true rates.

Stress and elongation data were recorded with a two-pen potentiometric recorder. The calibration was adjusted to give 10% elongation full scale and 10,000 or 20,000 psi stress full scale. Data values in excess of the full-scale ranges were recorded at constant sensitivity by offsetting the recorder zero one scale width, using calibrated potentiometric zero shifters. For some of the later tests, stress-strain plots were obtained during loading and unloading using an X-Y recorder driven by the

²The pyrolytic carbon shims in the holders were for testing annealed pyrolytic carbon where it was desired to clamp the specimen. They were not used for the glassy carbon tests.

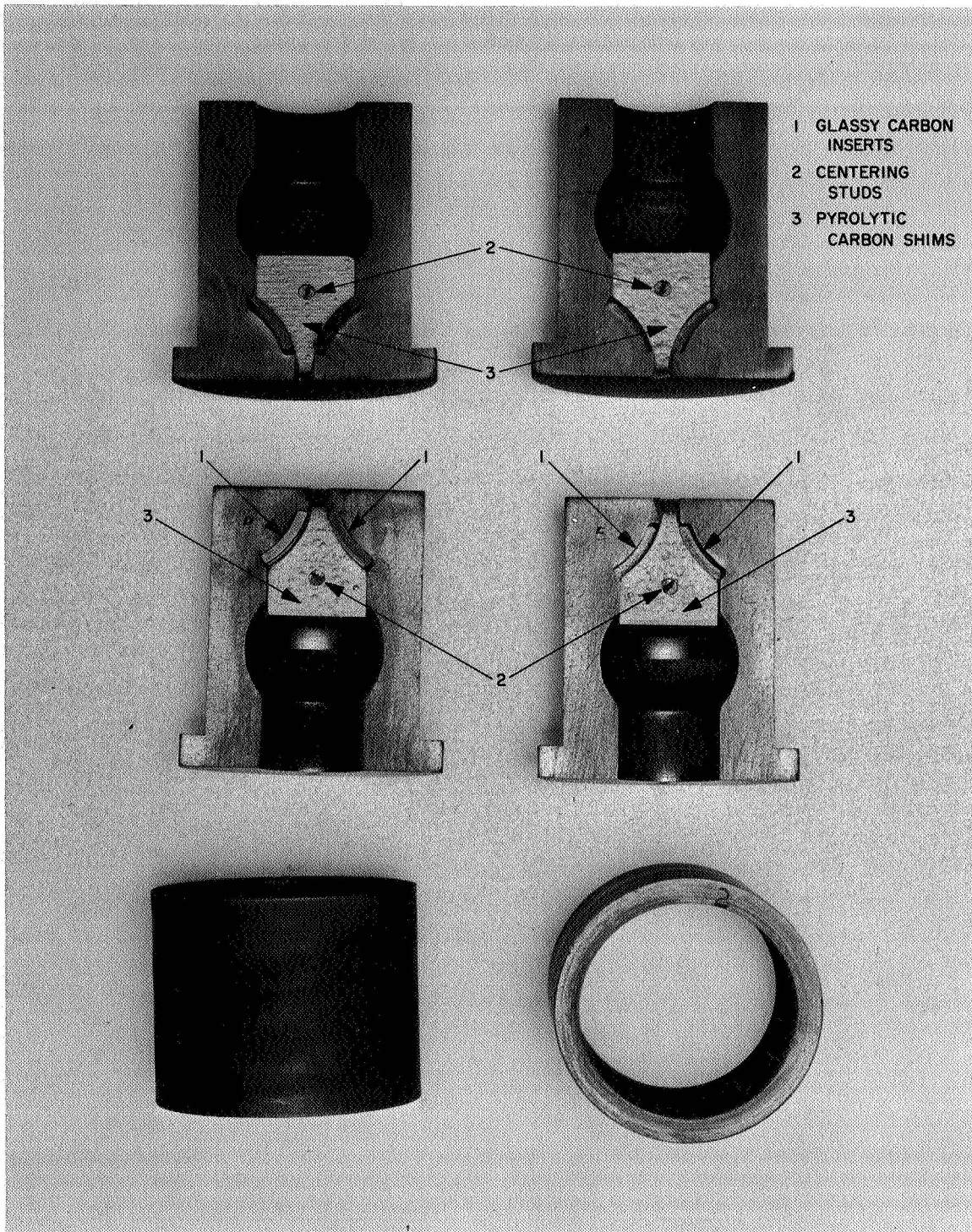


Fig. 1. Modified grip assembly showing GC-30 inserts, specimen centering screws and PC clamping shims, the latter not used

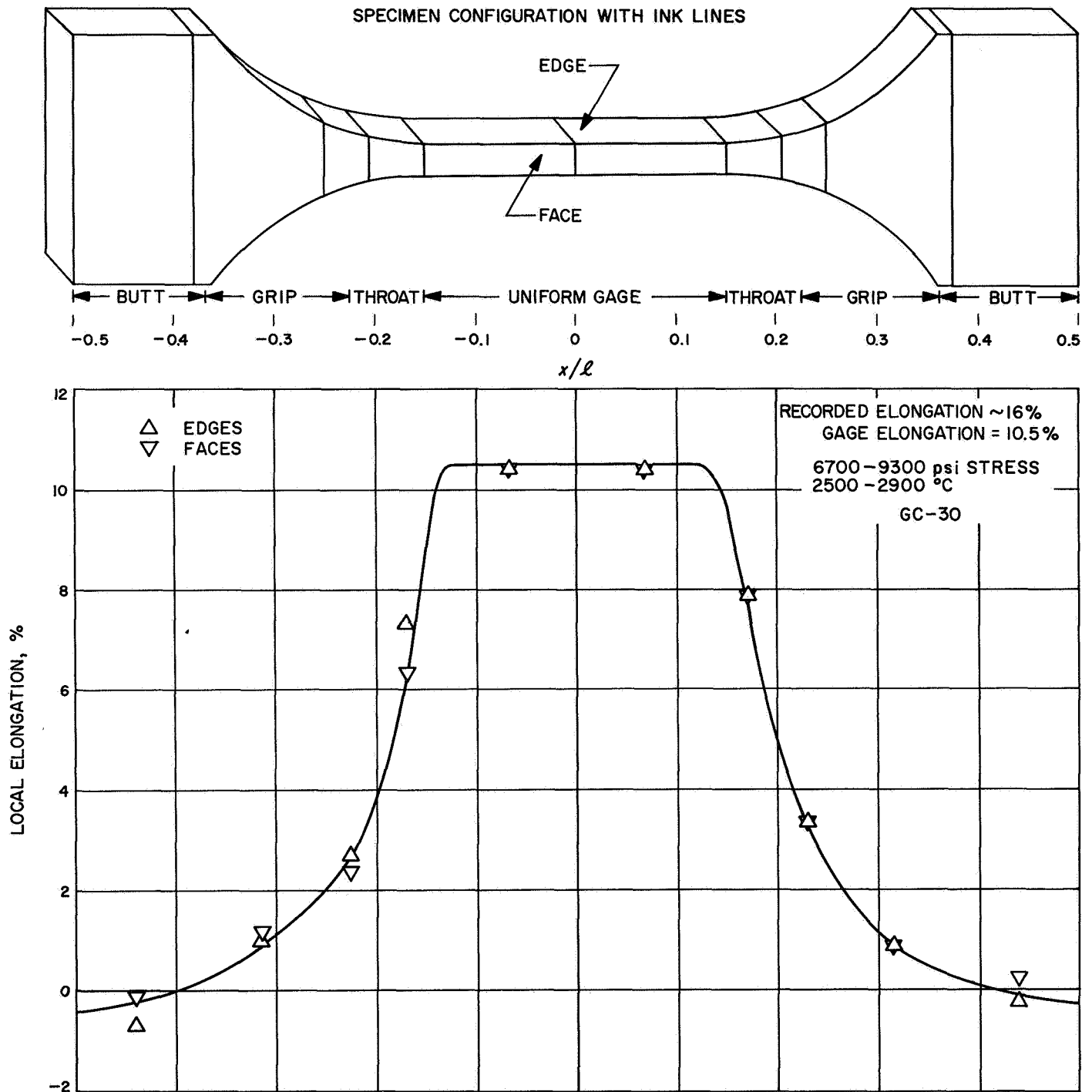


Fig. 2. Specimen configuration with ink fiducial marks, top, and observed distribution of deformation along specimen length, bottom

outputs of retransmitting slidewires on the primary two-pen recorder. Apparent static Young's modulus values at high temperatures could be obtained from these plots, but the results were of questionable significance because of the influence of small alignment changes when the load was changed, and uncertain values of the elasticity of the grips and the effective gage length and cross-sectional area. Similar results were obtained from the instantaneous elongations recorded by the two-pen recorder. Dynamic Young's modulus values were measured on several as-received glassy carbons at room temperature using a flexural resonant bar technique.

Magnetic susceptibility measurements were made by the Faraday method on samples cut from the gage sections of several deformed specimens. By measuring the susceptibility parallel and perpendicular to the stress axis, it was possible to determine the relative amount of layer-plane preferred orientation produced by the deformation. The apparatus and techniques have been described elsewhere (Ref. 14).

III. Results

The reduction in cross-sectional area accompanying the tensile elongation was determined from micrometer measurements of the gage section dimensions before and after the test. The percentage reductions in width and thickness were equal within experimental error, as would be expected for an isotropic material. The reduction in area as a function of true uniform gage elongation is shown in Fig. 3. The \times and $+$ symbols represent earlier tensile test data³ on GC-20 and GC-30 respectively. For these data the gage elongation was estimated from the recorded elongation. The squares and circles are the present results on GC-20 and GC-30 respectively where gage elongation was determined using ink fiducial marks. An appreciable reduction in area was observed for both materials, but the data for GC-30 fall closer to the theoretical constant volume values than do the GC-20 results. The diamond point corresponds to the second deformation of a GC-20 sample which had been elongated 5.5% at 2600°C in a prior test. After this pre-treatment, this sample behaved like GC-30.

Magnetic measurements provide a simple means of detecting preferred orientation textures in carbons and graphites because of the strong anisotropy of the diamagnetism (Ref. 15). The ratio, in graphite single crystals,

³Unpublished data of W. V. Kotlensky.

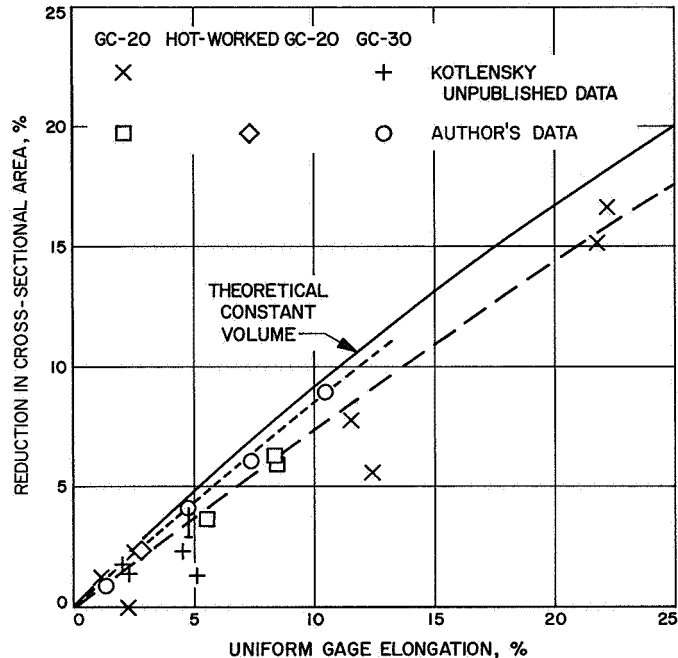


Fig. 3. Reduction in cross-sectional area as a function of uniform gage elongation for GC-20 and GC-30

of the diamagnetic susceptibility measured perpendicular to the layer planes to that measured parallel to the planes is about 70. In disordered carbons like glassy carbon this ratio is expected to be smaller, but still appreciably greater than unity. A discussion of the magnetic properties of glassy carbon as a function of heat treatment temperature and tensile deformation has been presented elsewhere (Ref. 16). In this investigation, magnetic susceptibility anisotropy ratio measurements were made on gage section samples from two GC-20 and two GC-30 specimens which had been deformed in tensile creep. The results are shown in Table 1. χ_l , χ_w and χ_t are the susceptibilities measured parallel to the length (parallel to the stress) and to the width and thickness

Table 1. Gage section magnetic susceptibility anisotropy ratios

Grade	Sample	Deformation temperature, °C	Gage elongation, %	χ_w / χ_t	$\chi_w, t / \chi_l$
GC-20	A	2600	8.5	1.00	1.20
GC-20	B	2600	8.5	1.01	1.19
GC-30	C	2600-2800	7.4	1.01	1.16
GC-30	D	2500-2900	10.5	1.00	1.25

(perpendicular to the stress) directions, respectively. The values of the anisotropy ratio χ_{10}/χ_t are unity, showing that the deformed material remains isotropic in the plane perpendicular to the stress axis. However, the anisotropy ratio $\chi_{(10,t)}/\chi_t$ is greater than one and the value increases approximately linearly with increasing gage elongation. This means that tensile deformation causes some alignment of the basal planes parallel to the stress axis. The observed anisotropy ratios for GC-20 and GC-30 appear to be the same function of the elongation. However, the deformation-induced orientation texture in GC-20 is probably a little stronger than that in GC-30 because the intrinsic anisotropy of the diamagnetism is believed to be larger in GC-30 than in GC-20.

The stress dependence of the creep rate $\dot{\epsilon}$ is commonly determined by measuring the steady state creep rate under various stresses σ , and expressed in terms of the stress exponent n using the empirical relationship

$$\dot{\epsilon} = A\sigma^n \quad (1)$$

where A is a proportionality constant. However, the creep rate of glassy carbon was found to decrease monotonically under constant load at constant temperature. No minimum rate or steady state creep region was observed. This behavior seems to be common to most carbons and graphites, including conventional coke-pitch graphites (Ref. 13) and pyrolytic carbons (Refs. 17 and 18).⁴ Since no steady state creep was observed, it was necessary to use a stress-change technique. At constant temperature, the sample was allowed to creep under a stress σ_1 until the "equilibrium" creep rate was established. Then the stress was abruptly increased or decreased to another stress level σ_2 and the creep rate again established. The stress was alternated over a range of values throughout the test. A portion of the elongation-time record for such a test on GC-30 at 2700°C is shown in Fig. 4. If no transient creep results from the stress change and Eq. (1) is obeyed, n may be determined from the slope of the linear plot of $\log \dot{\epsilon}_2/\dot{\epsilon}_1$ vs $\log \sigma_2/\sigma_1$ where $\dot{\epsilon}_1$ and $\dot{\epsilon}_2$ are respectively the creep rates immediately before and after the stress change (Refs. 19-22). It was found that, however, immediately after a stress increase, $\dot{\epsilon}$ was abnormally high; immediately after a stress decrease, the $\dot{\epsilon}$ was negative and passed through zero before finally assuming the "equilibrium" value appropriate to the stress and elongation, as shown in Fig. 4. Furthermore, the creep rate was a decreasing function

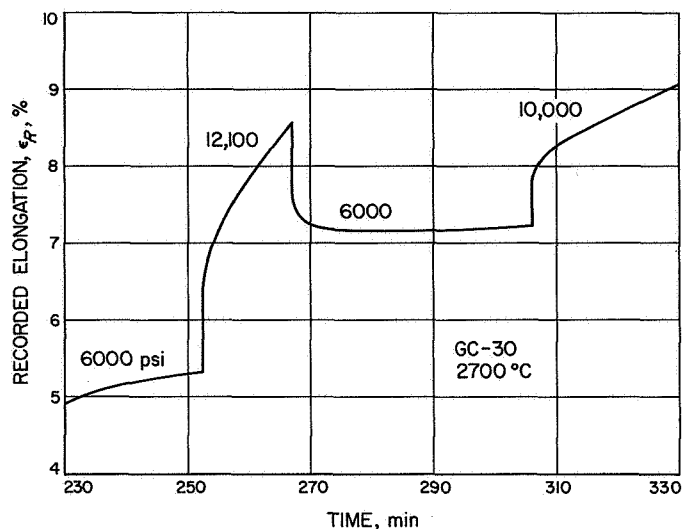


Fig. 4. Portion of a typical elongation vs time curve showing stress changes

of creep elongation as noted above. Finally, variation in behavior from specimen to specimen is a well known characteristic of carbons and graphites (and of high temperature tests) which makes the correlation of quantitative data from different specimens difficult.

For all of these reasons, special care is required in determining the influence of stress (or temperature) on the creep rate. Ideally, a family of creep rate vs creep elongation curves obtained under various stresses but otherwise identical conditions on a single sample would be desirable. From such a set of data, the stress dependence at constant creep strain could be determined. This ideal situation was approximated by periodically alternating the stress over a range as large as a factor of 18 during a single constant temperature test on a single specimen. In this way, curves of $\dot{\epsilon}$ vs creep elongation ϵ_c were obtained at several stress levels in a single creep run, as shown in Fig. 5. The numbers in brackets show the sequence in which the stress changes were made. The creep elongation ϵ_c was determined by subtracting the instantaneous quasi-elastic strain ϵ_e accompanying a stress change (heavy vertical lines in Fig. 4) from the recorded total elongation ϵ_R . On a plot of $\log \dot{\epsilon}$ vs $\log \epsilon_c$ (Fig. 5), the data plotted as a set of approximately parallel straight lines. In other words, the hardening rate $d \log \dot{\epsilon} / d \log \epsilon_c$ appeared to be independent of stress and elongation. The hardening rate also seemed to be approximately temperature-independent. Within experimental accuracy, at constant temperature, data points for a given stress level fell on the same line regardless of whether the stress had been increased or decreased.

⁴Also unpublished data of the author of this report.

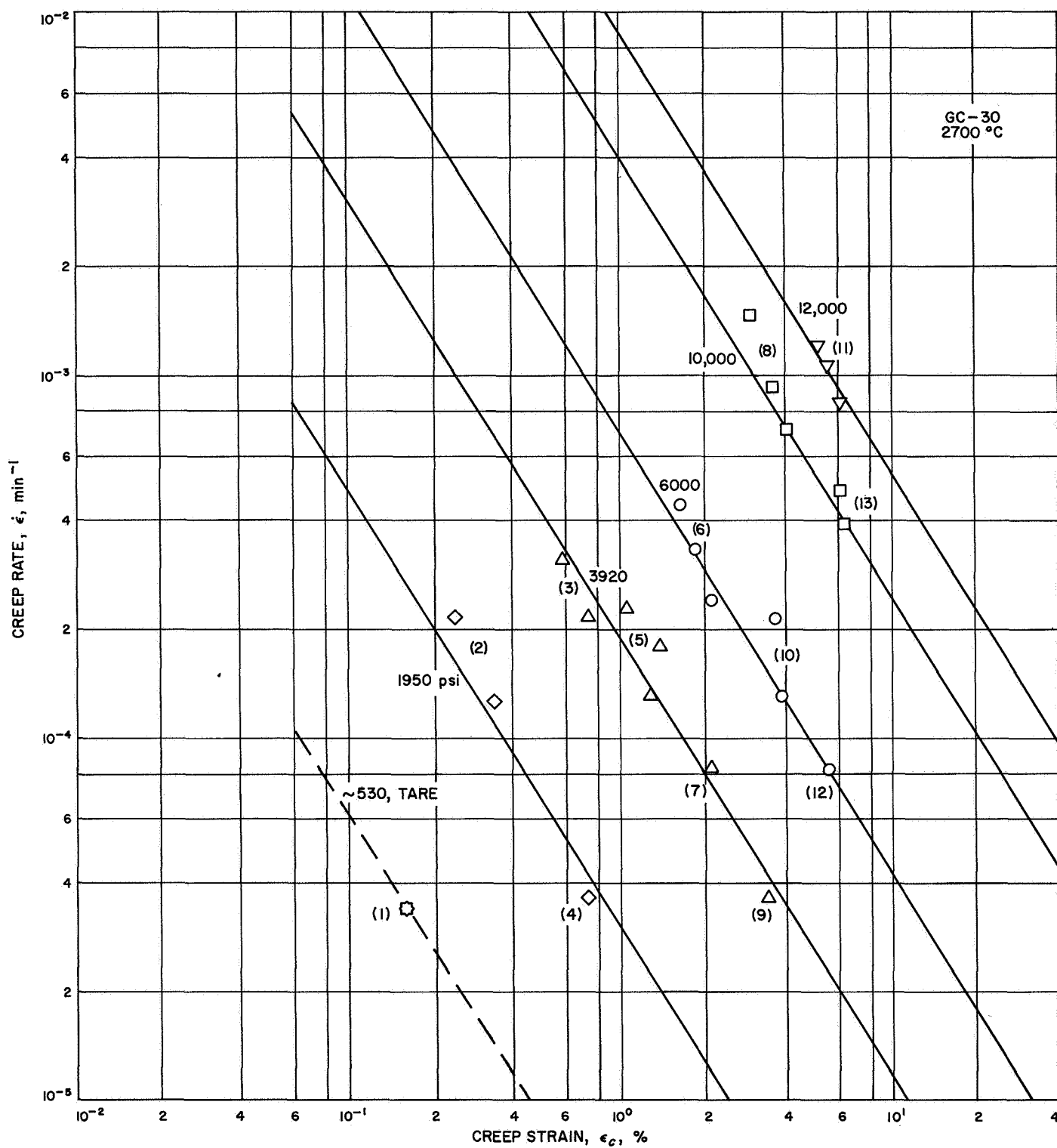


Fig. 5. Recorded creep rate as a function of creep elongation (log-log coordinates) for a GC-30 specimen at several stress levels

This behavior lends support to the assumption that this method does give the characteristic creep rates associated with each stress level. In general, clearly transient creep rates were not plotted in Fig. 5.

Once a set of data such as that in Fig. 5 has been obtained, it is a simple matter to determine the stress dependence by taking a vertical cut at the desired value of creep elongation. Since the $\log \dot{\epsilon}$ vs $\log \epsilon_c$ lines for different stresses are approximately parallel, the value of ϵ_c is not important, but it is prudent to choose an ϵ_c value which requires a minimum amount of extrapolation. A plot of $\log \dot{\epsilon}$ vs $\log \sigma$ at $\epsilon_c \sim 1\%$ obtained from Fig. 5 is shown in Fig. 6. The data points in the range 2000–12,000 psi can be fitted fairly well with a straight line of slope corresponding to a stress exponent value $n \sim 3.1$. This appears to be a good average value for n for glassy carbon in this stress range. However, the data in Fig. 6 show a definite positive curvature, even when the tare stress point at ~ 500 psi is excluded. Straight line segments between adjacent pairs of points give n

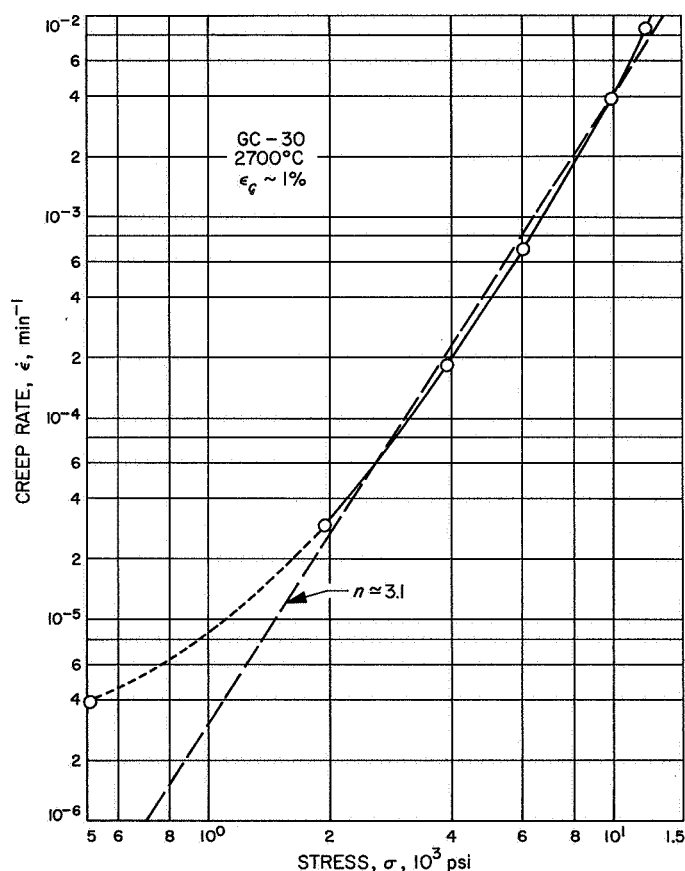


Fig. 6. Creep rate as a function of stress, from data of Fig. 5

values ranging from 1.5 for 500–2000 psi to 4.2 for 10,000–12,000 psi. Examination of all of the data obtained, at stresses ranging from 500 to 18,000 psi on various samples, confirms this trend as shown in Fig. 7 where the solid points indicate GC-30 and the open points indicate GC-20. The observed n values increase from ≤ 1.5 to ≥ 6.5 over this stress range, and no clear dependence on temperature is apparent. Equation (1) with n constant is therefore not a satisfactory description of the stress dependence of the creep rate in glassy carbon. However, the present results can be approximately fitted by Eq. (1) if $n = 1 + B\sigma$ where $B \simeq 3.7 \times 10^{-4} \text{ in.}^2/\text{lb}$, as shown by the straight line through the points in Fig. 7.

Dynamic Young's modulus measurements at room temperature on as-received material gave values of 3.57×10^6 psi for GC-30 and 4.07×10^6 for GC-20. A vitreous carbon reported by the manufacturer⁵ to have been heat-treated to a maximum temperature of about 1000°C had a modulus of 4.20×10^6 psi. Similar values have been reported by Taylor and Kline (Refs. 23 and 24). These results indicate a consistent decrease in modulus as the heat treatment temperature is increased. Static modulus values obtained with the creep apparatus ran

⁵Grade P6927, obtained from The Carbone Corporation, Boonton, N. J.

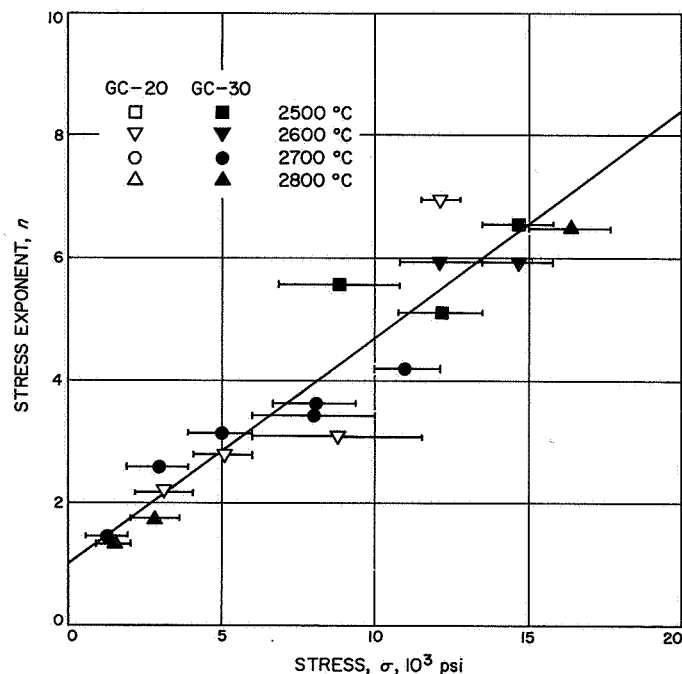


Fig. 7. The stress exponent n as a function of stress for GC-20 and GC-30

about 1×10^6 psi at both room and elevated temperatures after correction for reduction in area and effective gage length (using the factor found for plastic gage elongation). This is much lower than the dynamic modulus. The large difference is probably due largely to elasticity of the grips and an effective gage length correction which was inadequate for the elastic measurements. Instantaneous plastic deformation did not appear to have a major influence since similar values were obtained for stress increases and decreases. Probable variation of these effects with temperature and a large scatter range in the data prevented any determination of the temperature dependence of the modulus. There appeared to be some tendency for the apparent modulus to increase with elongation, however.

As shown in Fig. 4, a time dependent creep recovery occurs whenever the stress is decreased at elevated temperature. No extensive investigation was made of this effect, but it appeared to be a non-linear function of the stress reduction. Although only a small amount of recovery was observed when the load was partially removed, the amount of recovery on complete unloading was substantial. For example, a stress reduction from 12,000 to 6000 psi, after a recorded elongation of 8.5% at 2700°C, resulted in a recovery of about 0.5% elongation in 10 min (Fig. 4). However, reducing the stress by about 95% (13,780 to the 540 psi tare stress) at 2600°C after a recorded elongation of 10.2% in another specimen resulted in a recovery of about 1.8% elongation in 10 min despite the lower temperature, as shown in Fig. 8. In

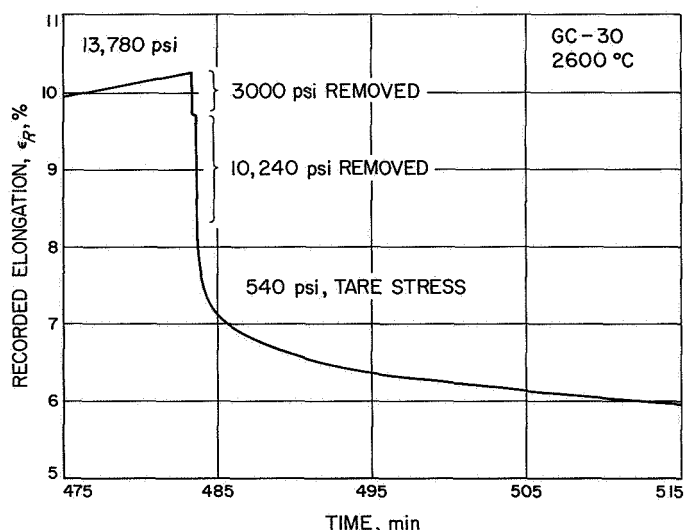


Fig. 8. Typical elongation vs time curve showing creep recovery when load was removed

part, of course, this is due to the fact that creep elongation continues when an appreciable stress remains on the sample. This does not appear to be sufficient to explain the difference since the creep rate is as much as an order of magnitude less than the recovery rate. On the other hand, low creep rates could result from partial cancellation by simultaneous recovery. However, this is not consistent with the observation that creep rates at a given stress level fall on the same curve whether the stress is increased or decreased to reach this level. A substantial portion of the total creep strain is recoverable under minimum stress conditions, as shown in Fig. 8. After 30 min at the test temperature of 2600°C under the tare stress, about 25% of the recorded creep elongation had recovered, and recovery was still continuing. The maximum recovery was not determined, nor was the temperature dependence of the recovery investigated.

The temperature dependence of the creep rate was determined by a technique similar to that used to study the stress dependence. The creep rate of a single specimen was observed as a function of creep strain under a constant load as the temperature was cycled over a range of values. The results of such a test on a GC-30 specimen over the range 2500–2900°C under a stress of 6700 psi are shown in Fig. 9. An Arrhenius plot of these data at constant creep elongation, shown in Fig. 10, gave an effective activation energy value of 360 kcal/mole. Temperature change experiments on other samples over more limited temperature ranges and at stress levels of 6000–16,000 psi gave energy values ranging from 306 to 382 with an average value of 350 kcal/mole. No correlation between energy and stress or elongation was apparent in this range. The effective activation energy for high temperature creep of glassy carbon therefore appears to be 350 ± 40 kcal/mole.

IV. Discussion

Despite its low bulk density of about 1.5 g/cm³ and isotropic structure, glassy carbon deforms at nearly constant volume, as indicated by the reduction in area results in Fig. 3. This contrasts with the behavior of conventional synthetic binder-filler carbons and graphites which generally show little reduction in area as a result of tensile deformation, regardless of density or preferred orientation.⁶ Because of the large reduction in

⁶An exception to this general rule is POCO graphite, a dense, fine-grained isotropic synthetic graphite which may have a thermosetting resin binder, as disclosed by G. V. Bennett, in a private communication.

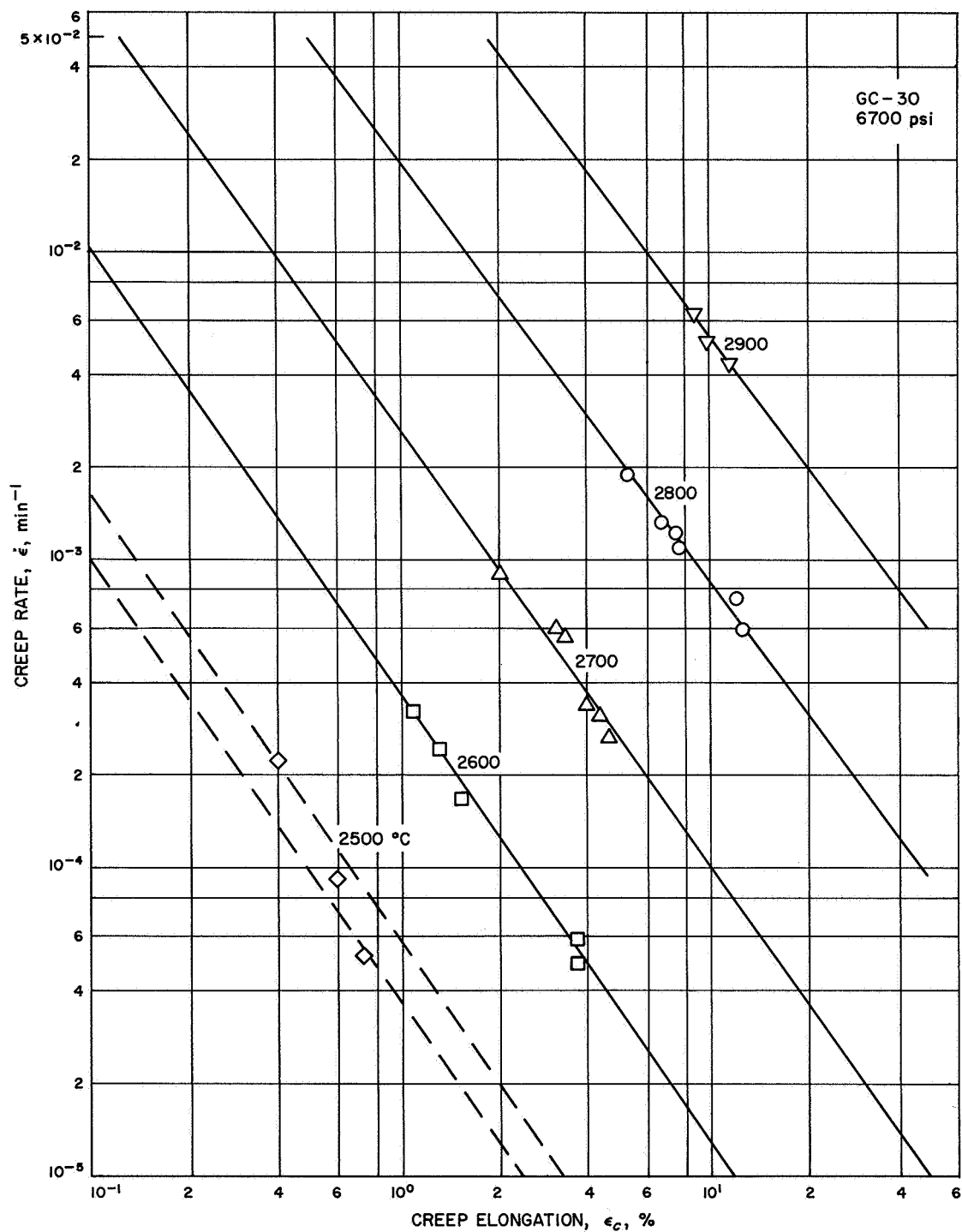


**Fig. 9. Recorded creep rate as function of elongation (log-log coordinates)
for a GC-30 specimen at several temperatures**

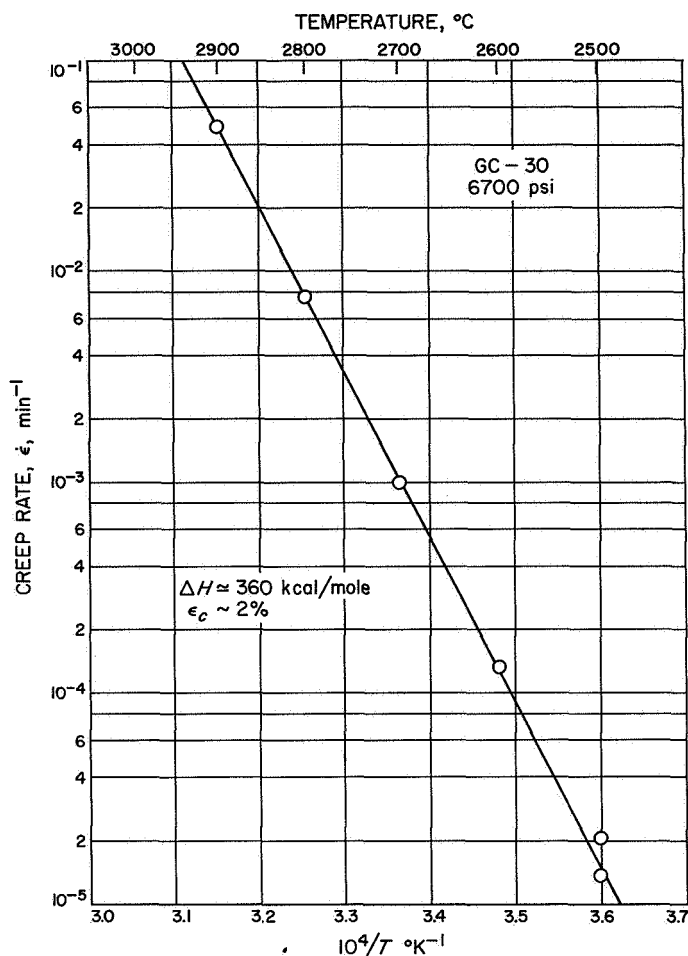


Fig. 10. Arrhenius plot of creep rate vs reciprocal absolute temperature, from data of Fig. 9

area, growth of cracks and pores cannot contribute significantly to the deformation of glassy carbon. The elongation is therefore truly plastic and must result from homogeneous deformation of the material. However, to account for the recovery, it may be partly anelastic. In tensile tests conducted at constant cross-head speed, the fracture elongation of GC-20 was found to be much greater than that of GC-30 at temperatures above about 2200°C (Refs. 9–11). However, if reduction in area is taken as the criterion, GC-30 is more ductile than GC-20. The low fracture elongation of GC-30 may therefore result at least in part from a strain-rate effect. The present reduction in area results for GC-20 is in general agreement with the reduction in bulk density observed in the earlier tensile investigation (Ref. 11).

The empirical representation of the stress dependence of the creep rate by an expression of the form $\dot{\epsilon} = A\sigma^n$, $n = 1 + B\sigma$ appears to have little physical significance.

It may be that the stress range covered here spans a transition region between two or more rate-determining deformation mechanisms. At very low stress, n appears to approach 1 and a viscous creep process such as Nabarro–Herring stress-directed diffusion creep (Refs. 25–27) may be involved. Such a mechanism is favored by the small crystallite size and disordered structure of glassy carbons. The theory indicates that for this mechanism at low stress, $\dot{\epsilon} = AD\sigma/d^2T$ where A is a constant, D is the self-diffusion coefficient, d is the crystallite diameter and T is the absolute temperature; at high stresses, $\dot{\epsilon} = (B/d^2) \sinh(CD\sigma/T)$ where B and C are constants. However, it is impossible to justify such a mechanism quantitatively without a detailed knowledge of crystallite size and shape, and self-diffusion. The observed stress dependence at high stresses does not appear to fit the sinh law when reasonable values are substituted for the parameters. Intuitively, it is difficult to understand the lack of influence of tensile deformation on the X-ray diffraction structure (Refs. 11 and 16) if stress-directed diffusion is a major contributor to the deformation. A low stress dependence has also been observed by the author in highly oriented, well-graphitized pyrolytic carbons stressed parallel to the layer planes, but here the detailed deformation mechanisms must certainly be different. The strong stress dependence observed in glassy carbons at high stress levels is equally difficult to explain. The high stress values of $n \geq 6$ are similar to those observed in conventional and stress-recrystallized binder-filler synthetic graphites (Refs. 19–22). The stress exponent appears to be approximately constant over a fairly broad stress range in these latter materials. Moreover, as discussed above, in binder-filler graphites the tensile reduction in area is generally small and the elongation appears to occur primarily by the growth of cracks and voids oriented parallel to the crystallite layer planes at least in well-oriented stress-recrystallized graphites (Refs. 21, 22, and 27). Some other deformation mechanism must operate in glassy carbon. Where dislocation climb is the rate-determining process, as in many metals, n values ≥ 4 are found. However, the highly disordered structure and small crystallite size ($\leq 100 \text{ \AA}$) of glassy carbon makes such a dislocation mechanism very unlikely in these materials. Other empirical laws, such as an exponential dependence of creep rate on stress, are well known for metals, especially at high stress levels. However, data such as that in Fig. 6 do not fit an exponential law either. On a $\log \dot{\epsilon}$ vs σ plot, these data show a pronounced negative curvature. This also appears to rule out a linear combination of σ^n and exponential terms. Evidently, a more detailed knowledge of the

structure and mechanical behavior of glassy carbon will be required before the stress dependence of the creep rate can be satisfactorily explained.

The high effective activation energy of about 350 kcal/mole for creep of glassy carbon is rather surprising. It is now well established that creep (Ref. 17), and as noted by the author, and other deformation processes (Ref. 28), as well as graphitization and the associated microstructural changes (Refs. 29 and 30) in pyrolytic carbons, have an activation energy of about 250 kcal/mole. The graphitization of other graphitizing carbons, such as coke-pitch composites (Ref. 31), also is controlled by this activation energy, and there is growing evidence that high temperature deformation processes such as creep have the same activation energy in these materials (Refs. 21 and 22). Based on both theoretical and experimental values for the energies required, plane vacancy diffusion appears to be the rate controlling process associated with the 250 kcal/mole activation energy in graphites and graphitizing carbons (Ref. 30). Theoretical considerations indicate that the activation energy for self-diffusion by an interstitialcy mechanism should be higher than that for vacancy diffusion in graphite because of the large formation energy of interstitial atoms (Ref. 32). Because of structural differences, the energy values and/or the operating diffusion mechanisms in nongraphitizing carbons may differ from those in graphitic materials. However, intuitively, it might be expected that lower energies would prevail in glassy carbon for diffusion by any defect mechanism because of its highly disordered and distorted structure. It is possible that the observed activation energy is only an apparent or effective value that cannot be directly related to the physical processes involved. All of the present temperature dependence data was obtained in the mid-to-high stress range: 6000–16,000 psi. Unfortunately, there does not appear to be any other information on deformation or diffusion activation energies in glassy carbons with which to compare the present results.

V. Structure of Glassy Carbon

The structure of glassy carbon is not understood in detail, and it is difficult to interpret the high temperature mechanical properties without this knowledge. On the other hand, the observed properties and behavior of glassy carbon may be used to infer a structural model. It is known that these materials are prepared from well cross-linked aromatic thermosetting resins. The pyrolysis is carried out slowly enough to permit the volatile prod-

ucts to escape by diffusion, and to allow the large shrinkage accompanying pyrolysis to be accommodated without cracking. These requirements place a limitation on the thickness of materials which can be prepared on a reasonable heat treatment time schedule. The maximum thickness in which Japanese glassy carbon has been commercially available is about $\frac{1}{8}$ in. The carbonization process is completed at or below 1000°C, but considerable internal stress, lattice distortion and carbon-carbon cross-link bonds must remain after treatment to this temperature. X-ray diffraction studies (Refs. 2, 11, 16, 33, and 34) confirm this supposition. After carbonization at 800–1000°C the diffraction pattern is very diffuse, the apparent crystallite size is very small, and the interlayer spacing and amount of "disorganized" carbon are large. Radial distribution studies (Refs. 33 and 34) suggest a mixture of trigonal (graphitic) and tetragonal (diamond-like) bonds. With heat treatment, especially at temperatures above 2000°C, the diffraction lines sharpen somewhat, the apparent crystallite size increases, and the interlayer spacing and disorganized carbon decrease. However, the graphitization process does not proceed very far. Even after 1 h at 3200°C, the X-ray structure is still that of a small-crystallite turbostratic carbon (Refs. 11 and 16). Both X-ray and magnetic susceptibility results indicate that glassy carbon consists of randomly oriented crystallites with a structure similar to those of graphitizing turbostratic carbons (Ref. 16).

Although the material as prepared is macroscopically isotropic, extensive tensile elongation of GC-20 at high temperature results in a pronounced preferred orientation texture, with the layer planes tending to lie parallel to the tensile axis. Tensile deformation has little or no influence on crystallite size or interlayer spacing. However, heat treatment under a hydrostatic pressure of 5–10 kilobars results in appreciable graphitization in short times at temperatures of 2600°C or below (Refs. 35–37).

The bulk density of glassy carbon is appreciably lower than can be accounted for on the basis of the X-ray lattice parameters and the visible macroscopic porosity. High temperature heat treatment causes little or no change in density. Recent small angle scattering studies⁷ have indicated the presence of appreciable microscopic porosity (maximum dimensions ≤ 100 Å). This microporosity, which can account for the low bulk density, apparently takes the form of voids and interstices between adjacent crystallites. High temperature tensile deformation causes the bulk density to decrease somewhat.

⁷In private communication of W. Ruland.

The room temperature dynamic modulus decreases by about 15% as the maximum treatment temperature goes from 1000 to 3000°C. Nevertheless, the Young's modulus remains very high for an isotropic carbon of low density (Refs. 38 and 39). It is about the same as that of as-deposited pyrolytic carbon parallel to the substrate. The indentation and scratch hardnesses are high, but decrease somewhat with heat treatment (Ref. 11). Although the fracture elongation of GC-30 is much lower than that of GC-20, the tensile strengths are approximately the same; and the strength is quite high, especially on a per unit weight basis. These results indicate that glassy carbon is very strongly bonded together. High temperature heat treatment causes some change in this bonding which affects the elastic and plastic behavior but has little effect on the strength.

These properties suggest the following simple structure model, which is an elaboration of the model proposed by Noda and Inagaki (Refs. 33 and 34). Small crystallites with a distorted and turbostratic lattice structure are randomly oriented and strongly bonded one to another. The lattice distortion results in part from defects of various sorts within the crystallites, and in part from distorted intercrystallite bonds. The high Young's modulus implies strong intercrystallite bonds and a high interlayer shear modulus within the crystallites. The shear modulus would be expected to be increased somewhat by the small crystallite size and by lattice defects within the crystallites which prevent dislocation bowing. However, lattice defects and disordered stacking with the attendant increase in interlayer spacing would be expected to reduce the intrinsic crystallite modulus. Therefore, it is necessary to postulate stronger interlayer bonding than in graphite, either by occasional direct c-c bonds (perhaps of the tetragonal type) or perhaps by bonded interstitials (Ref. 40).

Strong bonds between the crystallites are also necessary to explain the properties of glassy carbon. These must be primarily carbon-carbon bonds since it seems unlikely that sufficient quantities of hydrogen, oxygen or other impurities remain in the lattice after heat treatment at temperatures $\geq 2000^\circ\text{C}$. Both chemical analysis and magnetic susceptibility results indicate the substantial loss of metallic impurities like iron at temperatures below 2600°C (Ref. 16). Because of the random orientation of the crystallites, two general classes of intercrystallite bonds must be considered: Layer plane edge-to-edge bonds, and layer plane edge-to-layer plane face (or face-to-face) bonds. Simple plausibility suggests that the

edge-edge bonding should be the stronger and more common type, although such bonds would be strained and distorted by large angle twist and tilt misorientations between adjacent crystallites about axes perpendicular to the crystallite c-axes. These crystallite edge-to-edge bonds are considered to be the major source of the high macroscopic modulus, hardness and strength of glassy carbons. When considered in the context of the macroscopically isotropic structure, they must interconnect the crystallites into a complex, branched, tangled chain configuration.

The weaker, less frequent edge-to-face intercrystallite bonds, which may be either carbon-carbon or impurity links, should also contribute to the hardness and modulus of glassy carbons which have not been treated at high temperatures. As noted above, such carbons, as a result of shrinkage during pyrolysis, etc. probably have high internal stresses. At elevated temperatures, especially $>2000^\circ\text{C}$, a relaxation of the tangled chain structure may occur under the combined influences of frozen-in stresses, differential thermal-expansion stresses, and increased atomic mobility. In the process of this relaxation, the face-to-edge bonds are broken (if carbon-carbon) or lost by volatilization (if due to impurities). This results in a decrease in lattice distortion, hardness and modulus, but has little effect on density or tensile strength. If a tensile stress is applied during this relaxation process, large tensile elongations can be realized and the tangled crystallite chains tend to straighten out so that the individual crystallites tend to be oriented with their basal planes parallel to the stress axis. Intercrystalline voids created or enlarged in this process decrease the reduction of area and the density.

After treatment at elevated temperatures in the range 2600–3000°C, a more stable and relaxed bonding configuration has been established. The deformation process is similar to that described above, but it is more difficult to obtain large tensile elongations, and void formation and growth is reduced. Because of the random orientation texture and the distorted character of the intercrystallite bonding, an appreciable distribution of internal stresses will remain. The tensile deformation process must involve the stretching, bending, and ultimate breaking and reforming of the intercrystallite edge-to-edge type bonds. This process of bond rupture and reformation may be responsible for the high effective activation energy. Because of the distribution of internal stresses and bond configurations, a pronounced and monotonic hardening process occurs by an exhaustion mechanism as

elongation proceeds. As the "softer" bonds are used up (by distortion and reforming), the creep rate decreases and the apparent modulus increases. On removal of the stress, the energy stored in deformed bonds exerts a back stress producing the relaxation. However, this is opposed by bonds formed while the stress was applied. The new bond configuration formed under stress is able to withstand the small reverse stresses resulting from partial unloading; but the large reverse stresses produced by complete unloading result in appreciable reverse creep. This can account qualitatively for the time and stress dependence of the creep recovery.

VI. Summary

The tensile creep deformation of glassy carbon occurs at nearly constant volume, and has a high effective activation energy of about 350 kcal/mole. The creep rate decreases monotonically with elongation at a rate which is approximately independent of both stress and tem-

perature. A substantial fraction of the creep elongation is recoverable on removing the stress at high temperatures. The stress dependence of the creep rate is low, approaching a viscous law, at very low stresses. At high stresses, however, the stress exponent increases to $n \geq 6$. A structural model for glassy carbon consisting of small, distorted turbostratic crystallites strongly bonded together in a random tangled chain configuration has been hypothesized. This model can account qualitatively for many of the features of glassy carbon. Although the model seems consistent with what is known about the structure of glassy carbon, it was inferred from a catalogue of properties and there is little or no direct evidence for many of its specific features. It is obviously not advisable to push such hypothetical concepts too far in attempting to explain the detailed behavior of these materials. More detailed and direct information on the actual structure of glassy carbons is badly needed. In the meantime, the crude model proposed here may provide a basis for the qualitative discussion of the properties and behavior of these materials.

References

1. Yamada, S., and Sato, H., "Physical Properties of Glassy Carbon," *Nature*, Vol. 193, p. 261, 1962.
2. Yamada, S., Sato, H., and Ishii, T., "Eigenschaften und verwendung von glasartigen Kohlenstoff," *Carbon*, Vol. 2, pp. 253-260, 1964.
3. Porisot, J., "Vitreous Carbon," *Rev. Hautes Temp. Refract.*, Vol. I, p. 171, 1964.
4. Ishikawa, T., Teranishi, H., and Honda, H., "On the Physical Properties of Vitro Carbon," Paper P81, 8th Conference on Carbon, Buffalo, New York, June 1967.
5. Honda, T., Ohwada, K., Tateno, J., and Shimada, T., "Study on the Carbonization of Phenol-furfural Resin," Japan Atomic Research Institute Memo. 1518, Feb. 1964.
6. Fitzer, E., Schafer, W., and Yamada, S., "The Formation of Glass-like Carbons by Pyrolysis of Non-melting Resins," Paper P82, 8th Conference on Carbon, Buffalo, New York, June 1967.
7. Bradshaw, W., Pinoli, P., Watsey, G., and Wigton, H., "Fabrication Factors Affecting the Properties of Glassy Carbon," Paper P80, 8th Conference on Carbon, Buffalo, New York, June 1967.

References (contd)

8. Yamada, S., and Yamamoto, M., "A Tentative Preparation of Glassy Carbon Monofilament from Thermo-Setting Resin," Paper P83, 8th Conference on Carbon, Buffalo, New York, June 1967.
9. Kotlensky, W. V., and Martens, H. E., "Tensile Behavior of Glassy Carbon at Temperatures up to 2900°C," Paper V-2, Symposium on Carbon, Tokyo, Japan, 1964.
10. Kotlensky, W. V., and Martens, H. E., "Tensile Properties of Glassy Carbon to 2900°C," *Nature*, Vol. 206, pp. 1246-1247, 1965.
11. Kotlensky, W. V., and Fischbach, D. B., *Tensile and Structural Properties of Glassy Carbon*, Technical Report 32-842. Jet Propulsion Laboratory, Pasadena, Calif., Nov. 15, 1965.
12. Kotlensky, W. V., and Martens, H. E., *Tensile Properties of Pyrolytic Graphite to 5000°F*, Technical Report 32-71. Jet Propulsion Laboratory, Pasadena, Calif., March 10, 1961; also in *High Temperature Materials II*, AIME Met. Soc. Conf., Vol. 18, pp. 403-418. Edited by G. M. Ault, W. F. Barclay and H. P. Musinger. Interscience Publishers, Div. of John Wiley & Sons, New York, 1963.
13. Martens, H. E., Button, D. D., Fischbach, D. B., and Jaffe, L. D., "Tensile and Creep Behavior of Graphites Above 3000°F," Proceedings 4th Conference on Carbon, pp. 511-530. Pergamon Press, New York, 1960.
14. Fischbach, D. B., "The Magnetic Susceptibility of Pyrolytic Carbons," Proceedings 5th Conference on Carbon, Vol. II, pp. 27-36. Pergamon Press, New York, 1963; reprints released as Technical Report 32-165. Jet Propulsion Laboratory, Pasadena, Calif., March 1963.
15. Fischbach, D. B., "Effect of Plastic Deformation on Preferred Orientation of Synthetic Carbons," in *Supporting Research and Advanced Development*, Space Programs Summary 37-31, Vol. IV, pp. 29-31. Jet Propulsion Laboratory, Pasadena, Calif., June 30, 1964.
16. Fischbach, D. B., *Magnetic Susceptibility of Glassy Carbon*, Technical Report 32-1151. Jet Propulsion Laboratory, Pasadena, Calif., to be published. Also, to be published in *Carbon*.
17. Kotlensky, W. V., "Analysis of High Temperature Creep in Pyrolytic Carbon," *Carbon*, Vol. 4, pp. 209-214, 1966; also in Technical Report 32-889. Jet Propulsion Laboratory, Pasadena, Calif., Feb. 15, 1966.
18. Kotlensky, W. V., and Martens, H. E., "Mechanical Properties of Pyrolytic Graphite to 2800°C," Proceedings 5th Conference on Carbon, Vol. II, pp. 625-638. Pergamon Press, New York, 1963.
19. Green, W. V., and Zukas, E. G., "The Stress Dependence of the Creep Rate of Two Commercial Graphites," *Electrochem. Tech.*, Vol. 5, pp. 203-206, 1967.
20. Green, W. V., "The Stress-Dependence of the Creep Rate of a Uranium-Loaded Graphite," *Carbon*, Vol. 4, pp. 81-84, 1966.

References (contd)

21. Zukas, E. G., and Green, W. V., "The High Temperature Creep Behavior of a Heavily Oriented Graphite," Paper MI45, 8th Conference on Carbon, Buffalo, New York, June 1967.
22. Zukas, E. G., and Green, W. V., "Dependence of Rate of Creep on Orientation of the Tensile Axis for Heavily Oriented Graphite," *Nature*, Vol. 212, pp. 1455-1456, 1966.
23. Taylor, R. E., Kline, D. E., and Walker, P. L., Jr., "Dynamic Mechanical Properties of Graphite," Paper MI38, 8th Conference on Carbon, Buffalo, New York, June 1967.
24. Taylor, R. E., and Kline, D. E., "Internal Friction and Elastic Modulus Behavior of Vitreous Carbon From 4°K to 570°K." To be published, in *Carbon*.
25. Nabarro, F. R. N., "Deformation of Crystals by the Motion of Single Ions," pp. 75-90. Report of a Conference on the Strength of Solids, Physical Society, London, 1948.
26. Herring, C., "Diffusional Viscosity of a Polycrystalline Solid," *J. Appl. Phys.*, Vol. 21, pp. 437-445, 1950.
27. Dorn, J. E., and Mote, J. D., "Physical Aspects of Creep," *High Temperature Structures & Materials*, pp. 95-168. Edited by A. M. Freudenthal, B. A. Boley and H. Liebowitz. The MacMillan Company, New York, 1964.
28. Fischbach, D. B., and Kotlensky, W. V., "On the Mechanisms of High-Temperature Plastic Deformation in Pyrolytic Carbons," *Electrochem. Tech.*, Vol. 5, pp. 207-213, 1967.
29. Fischbach, D. B., "Kinetics of High-Temperature Structural Transformation in Pyrolytic Carbons," *Applied Phys. Letters*, Vol. 3, pp. 168-170, 1963.
30. Fischbach, D. B., *Kinetics of Graphitization. I. The High-Temperature Structural Transformation in Pyrolytic Carbons*, Technical Report 32-532. Jet Propulsion Laboratory, Pasadena, Calif., Feb. 1, 1966.
31. Fischbach, D. B., "Kinetics of Graphitization of a Petroleum Coke," *Nature*, Vol. 200, pp. 1281-1283, 1963; also released as Technical Report 32-570. Jet Propulsion Laboratory, Pasadena, Calif., Dec. 28, 1963.
32. Dienes, G. J., "Mechanism for Self-Diffusion in Graphite," *J. Appl. Phys.*, Vol. 23, pp. 1194-1200, 1952.
33. Noda, T., and Inagaki, M., "Structure of Glassy Carbon," Paper III-10, Symposium on Carbon, Tokyo, Japan, 1964.
34. Noda, T., and Inagaki, M., "The Structure of Glassy Carbon," *Bull. Chem. Soc. Japan*, Vol. 37, pp. 1534-1538, 1964.
35. Noda, T., and Kato, H., "Heat Treatment of Carbon Under High Pressure," Paper III-19, Symposium on Carbon, Tokyo, Japan, 1964.
36. Noda, T., and Kato, H., "Heat Treatment of Carbon Under High Pressure," *Carbon*, Vol. 3, pp. 289-297, 1965.

References (contd)

37. Noda, T., "Graphitization of Carbon Under High Pressure," Paper 1, 8th Conference on Carbon, Buffalo, New York, June 1967.
38. Fischbach, D. B., "Dependence of Mechanical Properties on Microstructure (of Carbons and Graphites)," in *Supporting Research and Advanced Development*, Space Programs Summary 37-41, Vol. IV, pp. 54-75. Jet Propulsion Laboratory, Pasadena, Calif., October 31, 1966.
39. Price, R. J., "Young's Modulus of Pyrolytic Carbon in Relation to Preferred Orientation," *Phil. Mag.*, Vol. 12, p. 561, 1965.
40. Wallace, P. R., "Configuration of Interstitial Atoms in Irradiated Graphite," *Solid State Comm.*, Vol. 4, pp. 521-524, 1966.